Original Article

Tissue Inhibitor of Metalloproteinase-3 Plays Important Roles in the Kidney Following Unilateral Ureteral Obstruction

Hidenobu KAWAMOTO[1)], Osamu YASUDA[1)], Takashi SUZUKI[2)], Tohru OZAKI[3)], Takamori YOTSUI[1)], Masayoshi HIGUCHI[1)], Hiromi RAKUGI[1)], Keisuke FUKUO[4)], Toshio OGIHARA[1)], and Nobuyo MAEDA[2)]

Tissue inhibitor of metalloproteinase-3 (Timp-3), an inhibitor of matrix-degrading enzymes, is an important molecule for maintenance of the extracellular matrix. In this study, we generated Timp-3–deficient mice and used them to examine the effect of Timp-3-deficiency on blood pressure and to investigate the role of Timp-3 in the kidney following unilateral ureteral obstruction. The blood pressure and heart rate of Timp-3–deficient mice were not significantly different from those of wild-type mice. On the other hand, the obstructed kidneys of Timp-3–deficient mice developed more severe hydronephrosis than those of wild-type animals. Matrix metalloproteinase activities assessed by *in situ* zymography and transforming growth factor-β expression were elevated in Timp-3–deficient mice. The renal tissues were thinner and the ratio of renal medulla to cortex was significantly lower in the obstructed Timp-3–deficient kidneys. These findings indicate that Timp-3-deficiency does not substantially affect the blood pressure in mice, and that Timp-3 plays an important role in the maintenance of renal macrostructure after unilateral ureteral obstruction. (*Hypertens Res* 2006; 29: 285–294)

***Key Words*: extracellular matrix, matrix metalloproteinase, hydronephrosis, tissue inhibitor of metalloproteinase-3, unilateral ureteral obstruction**

Introduction

Extracellular matrix (ECM) is an important component of every tissue, and is maintained by both the synthesis of new ECM components and the degradation of existing ECM (*1*). The degradation of ECM is mainly catalyzed by matrix metalloproteinases (MMP), which include collagenases, elastases, stromelysin and membrane-type MMP. The activity of MMP is tightly regulated in at least three steps, transcription, activation and inhibition. Tissue inhibitor of metalloproteinases (Timp), which consists at present of Timp-1, -2, -3, and -4 in mammals, is a physiological inhibitor of MMP. These inhibitors can potentially protect animals from pathological conditions caused by the overactivation of MMP, such as rheumatoid arthritis and rupture of atherosclerotic plaque (*2–4*).

Of the four Timp members, Timp-3, which was originally isolated from chicken fibroblasts (*5*), is unique in that it binds firmly to the ECM (*6*, *7*). Through this interaction, Timp-3 is localized where it can inhibit MMP activity. Unlike other Timp family members, Timp-3 inhibits tumor necrosis factor

From the [1)]Department of Geriatric Medicine, Osaka University Medical School, Suita, Japan; [2)]Department of Pathology and Laboratory Medicine, School of Medicine, the University of North Carolina at Chapel Hill, Chapel Hill, USA; [3)]Astellas Pharma Inc., Osaka, Japan; and [4)]Department of Food Sciences and Nutrition, School of Human Environmental Sciences, Mukogawa Women's University, Nishinomiya, Japan.

Address for Reprints: Osamu Yasuda, M.D., Ph.D., Department of Geriatric Medicine, Osaka University Medical School, 2–2 Yamadaoka, Suita 565–0871, Japan. E-mail: yasuda@geriat.med.osaka-u.ac.jp

Received January 12, 2006; Accepted in revised form January 17, 2006.

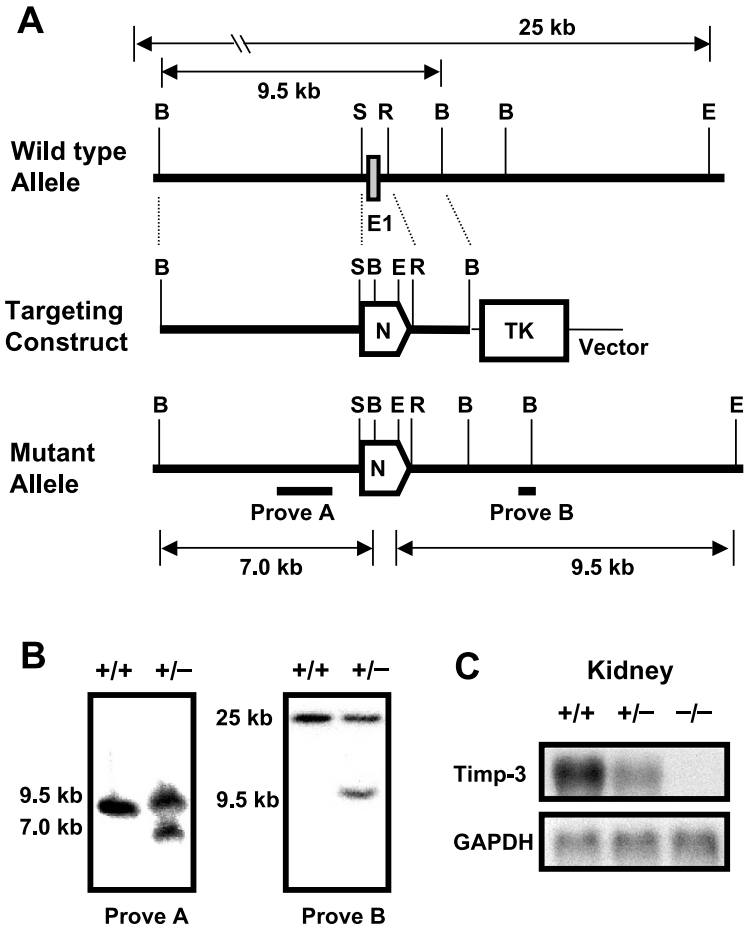

Fig. 1. *Targeted modification of the mouse* Timp-3 *gene. A: Schematic representation of the endogenous mouse* Timp-3 *allele, targeting vector, and mutant allele. The restriction enzyme cleavage sites used to construct the targeting vector and Southern blot analysis are shown. The thick horizontal line indicates genomic DNA containing exon 1. The probe used for Southern blot analysis is shown below the mutant allele. B, BamHI; E, EcoRI; R, EcoRV; S, SacII. B: Confirmation of the targeted allele by Southern blot analysis. Genomic DNA from* Timp-3$^{+/-}$ *or* Timp-3$^{+/+}$ *mice was digested with Bam HI or EcoRI and hybridized with probe A or B shown in A. Probes A and B detect 7.0- and 9.5-kb targeted fragments in addition to 9.5- and 25-kb endogenous fragments in correctly modified ES cells, respectively. C: Northern blot analysis of RNA (10 μg) isolated from kidneys of male mice of the three* Timp-3 *genotypes. The filter was hybridized with a Timp-3 probe (upper panel), washed, and rehybridized with a glyceraldehyde-3-phosphate dehydrogenase gene (GAPDH) probe (lower panel).*

α converting enzyme (TACE) (*8*), a metalloproteinase that is not a member of the MMP family. Recently, Timp-3 was reported to have functions in addition to inhibition of metalloproteinases. For example, Timp-3 inhibits the growth of tumor cells (*9*), and deficiency of Timp-3 in hosts was found to enhance tumor growth (*10*). Timp-3 is also reported to have an apoptosis-inducing activity (*11–13*) and anti-angiogenic activity by blocking the binding of vascular endothelial growth factor (VEGF) to VEGF receptor-2 (*14*). Interestingly, mutations of the *Timp-3* gene causes an autosomal dominant disease, Sorsby's dystrophy, which is characterized by the loss of central vision due to age-related macular degeneration (*15*, *16*).

Unilateral ureteral obstruction (UUO) is a model of renal fibrosis that mimics many aspects of obstructive nephropathy, including cellular infiltration, tubular proliferation and apoptosis, myofibroblast accumulation and increased ECM deposition (*17–19*). Some genetically engineered mice that are considered to influence the degradation of ECM have been studied by UUO. For example, plasminogen activator inhibitor-1 (PAI-1)–deficient mice had reduced interstitial fibrosis after UUO, although neither renal plasminogen activator nor plasmin activities were increased. In this model, PAI-1 is thought to play a role in the recruitment of fibrosis-inducing cells, including myofibroblasts and macrophages (*20*). In contrast, while the expression of Timp-1, a member of the Timp family, is increased after UUO (*21*), Timp-1-deficiency did not affect the interstitial fibrosis in a murine model of

UUO. This may have been due to the compensation by other Timp family members or PAI-1, or because inhibition of intrinsic MMP activity does not constitute a profibrogenic event in the kidney (*22*).

In the present study, we hypothesized that Timp-3 is implicated in the regulation of blood pressure through perivascular fibrosis and resistance, and plays an important role in the kidney, since Timp-3 is expressed at the highest level in the kidney in mice (*6*). To test this hypothesis, we generated Timp-3–deficient mice using gene targeting in embryonic stem (ES) cells. We found that, although blood pressure was not affected by Timp-3-deficiency, obstruction of Timp-3–deficient kidneys led to the development of severe hydronephrosis, and the ratio of medulla to cortex thickness was significantly reduced compared to that in the wild-type (WT) kidneys. These data indicate that Timp-3 plays roles in the maintenance of the renal macrostructure of after UUO.

Methods

Generation of Timp-3$^{-/-}$ Mice

A lambda phage clone containing exon 1 of the endogenous *Timp-3* gene was cloned using published sequences (*6*, *23*). The targeting vector was designed to replace exon 1 and the promoter region with a neomycin resistance gene (Neo). A 6.5-kb BamHI/SacII fragment in the 5′ upstream region of exon 1 provided a 5′ arm of homology, and a 1.8-kb EcoRV/BamHI fragment in intron 1 formed a 3′ arm of homology as illustrated in Fig. 1A. The targeting vector was linearized and electroporated into mouse ES cells derived from mouse strain 129/Ola. Colonies surviving after selection with G418 and ganciclovir were first screened by polymerase chain reaction (PCR) with primer F (5′-CTTCTATCGCCTTCTTGACG-3′) from the 3′ end of the Neo gene and primer R (5′-CACCCA CACCTCCCATTTTT-3′) from the 3′ portion of the BamHI site within intron 1. Positive clones that generated a 2.0-kb PCR fragment were expanded and confirmed by Southern blot analysis of BamHI-digested ES cell genomic DNA with a probe specific to the upstream portion of exon 1 or EcoRI-digested DNA with a probe specific to intron 1.

Mice and Genotyping

The ES cells with a correctly targeted *Timp-3* locus were injected into C57BL/6 recipient blastocysts. Chimeras were generated as described previously (*24*), and mated with C57BL/6 mice. Genotypes of mice were determined by PCR of tail DNA with three primers, Neo-F (5′-TGACCGCTTCT TCGTGCTTT-3′), Timp-3-F (5′-GGCTTGGGCTTGTCG GCTC-3′), and Timp-3-R (5′-CTCTCACCCTCCTTCTC CAG-3′). The 300-bp fragment amplified with Timp-3-F and Timp-3-R was derived from the normal allele, and the 230-bp fragment generated with Neo-F and Timp-3-R detected the targeted locus. Mice carrying the mutant allele were backcrossed with C57BL/6 mice more than seven times to produce the genetic background of C57BL/6.

Blood Pressure

Blood pressure and pulse rate were serially determined in conscious, trained mice using a non-invasive tail-cuff device.

RNA Isolation and Northern Blotting

Kidney RNA was isolated by using Isogen reagent (Nippon Gene, Tokyo, Japan). Northern blot analyses were performed by conventional methods, using probes for Timp-3, glyceraldehyde-3-phosphate dehydrogenase (GAPDH) and transforming growth factor-β (TGF-β) generated by reverse transcription-PCR of the RNA isolated from WT kidneys. The primer sequences used for the amplification of cDNA probes were Timp-3-F (5′-CAATTACCGCTACCACCTGG-3′) and Timp-3-R (5′-GGTGTATACATGCCTCGTTCC-3′) for Timp-3, GAPDH-F (5′-AAATGGTGAAGGTCGGTG TG-3′) and GAPDH-R (5′-GCAGAAGGGGCGGAGATG AT-3′) for GAPDH, and TGF-β-F (5′-ACCGCAACA ACGCCATCTAT-3′)and TGF-β-R (5′-ACTTCCAAC CCAGGTCCTTC-3′) for TGF-β. Probes were radiolabeled with [α^{32}P]dCTP using a Random Primer DNA Labeling Kit (Takara, Ohtsu, Japan).

Unilateral Ureteral Obstruction

Male Timp-3–deficient mice (KO) and WT C57BL/6 mice weighing 25–30 g were used. After induction of general anesthesia by the intraperitoneal injection of ketamine chloride (80 mg/kg) and xyladine sulfate (8 mg/kg), the mice were subjected to UUO as described elsewhere (*25–27*). Briefly, the left ureter was identified through a small abdominal incision and ligated with 6–0 silk suture. The experimental protocols were approved by the Osaka University Medical School Animal Care and Use Committee and were performed according to the Osaka University Medical School Guidelines for the Care and Use of Laboratory Animals.

Morphometric Analysis of the Kidney

Mice were sacrificed with an overdose of pentobarbital at 7 days after UUO. The kidneys were removed, photographed, and fixed in 4% paraformaldehyde (pH 7.4). Fixed tissues were placed in Tissue-Tek OCT embedding medium (Miles, Elkhart, USA), sectioned, and then stained with hematoxylin-eosin or Masson Trichrome staining reagents. To identify myofibroblasts, a monoclonal antibody against α-smooth muscle actin (α-SMA; DAKO, Glostrup, Denmark) was used, followed by an Avidin-Biotin coupling (ABC) immunoperoxidase technique, using a commercial kit (Vectastain Elite; Vector Laboratories, Burlingame, USA). Immunoreactive signals for α-SMA were scored in a blind fashion in at

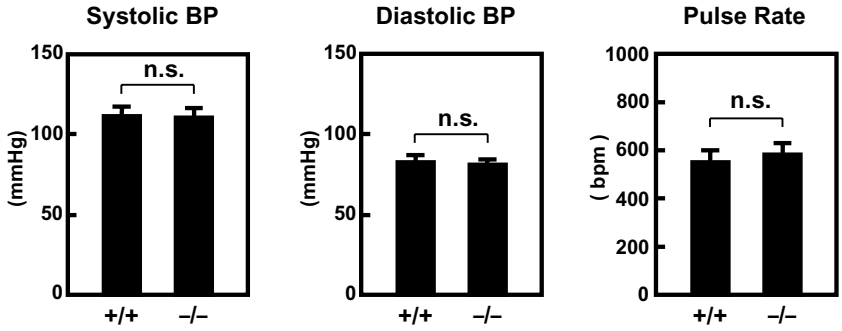

Fig. 2. *Effect of Timp-3-deficiency on blood pressure. Systolic and diastolic blood pressure were determined by the non-invasive tail cuff method. Columns and bars represent the mean±SD. BP, blood pressure.*

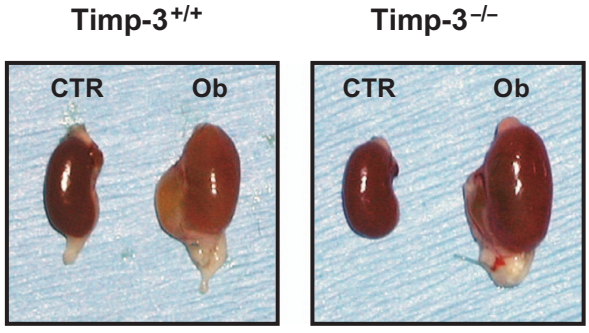

Fig. 3. *Photographs of the wild-type (Timp-3$^{+/+}$) and knockout (Timp-3$^{-/-}$) kidneys at 7 days after unilateral ureteral obstruction. CTR, control; Ob, obstructed.*

least 20 randomly chosen non-overlapping high power fields (×400) and were scored using the scale of 0 (absent), 1 (mild), 2 (moderate), and 3 (severe) (*28*).

In Situ Zymography

Fresh kidney tissue specimens were embedded without fixation in Tissue-Tek OCT compound (Miles). Frozen 10 μm sections were prepared using a cryostat and mounted onto films coated with 7% gelatin solution (Fuji Photo Film Co., Tokyo, Japan) as described (*29*). The film was incubated in a humidified chamber at 37°C for 1 h, and the specimens were stained with Biebrich Scarlet Stain Solution (Wako, Osaka, Japan) according to the manufacturer's instructions. Destained lesions, visualized by light microscopy, indicated gelatinolytic activity. As a control, we used gelatin films coated with 1,10-phenanthroline, an MMP inhibitor.

Statistical Analysis

Statistical analysis was performed using Student's unpaired *t*-test. Results are expressed as the mean±SD.

Results

Generation of Timp-3–Deficient Mice

Exon 1 and the promoter region of the *Timp-3* gene were deleted and replaced with the Neo gene by homologous recombination between the targeting vector and the endogenous *Timp-3* gene (Fig. 1A). Correctly targeted ES cells carrying the disrupted *Timp-3* gene were screened by PCR as described in the Methods section and confirmed by Southern blotting (Fig. 1B). The modified *Timp-3* locus showed 7.0-kb and 9.5-kb bands with probes, A and B, that are specific for 5′ and 3′ to the deleted DNA segment, respectively. The 9.5-kb band hybridizing to probe A and 25-kb band hybridizing to probe B indicate the endogenous gene. The lack of *Timp-3* gene expression in mice homozygous for the disrupted gene (KO) was confirmed by Northern blotting as illustrated in Fig. 1C. The expression levels in heterozygotes were about one half of those in WT mice.

Blood Pressure and Pulse Rate of Timp-3–Deficient Mice

To examine the potential role of Timp-3 on vascular resistance, blood pressure was determined by the tail-cuff method. As shown in Fig. 2, arterial systolic and diastolic blood pressures did not show significant differences between the WT (111±6/82±5 mmHg) and KO (110±7/81±4 mmHg) groups. Pulse rate was also not significantly different between WT (552±47 bpm) and KO (580±51 bpm) mice.

Macrostructural Changes in the Obstructed Kidneys

The left ureters of WT and KO mice were ligated as described in the Methods section, and right kidneys were used as controls. At 7 days after the UUO, the obstructed kidneys from KO animals were larger than those from WT mice (Fig. 3). To investigate whether the kidneys of KO mice were hyper-

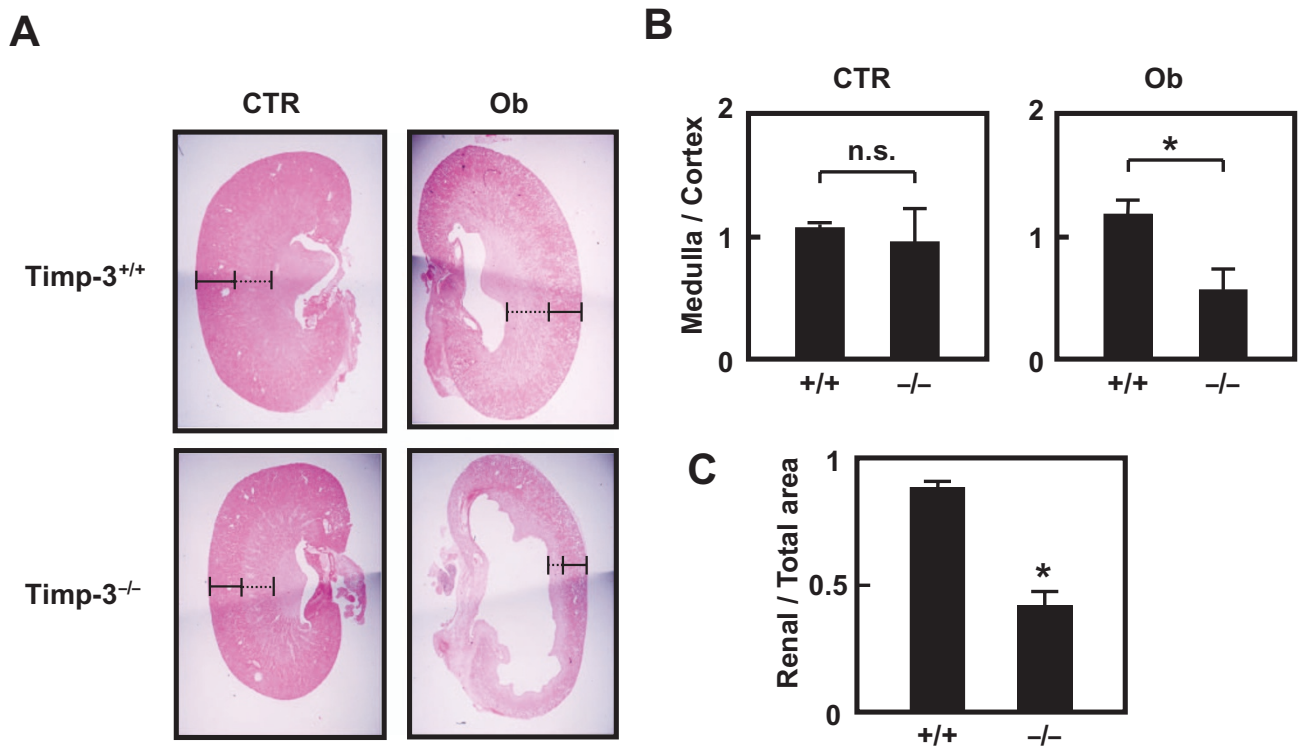

Fig. 4. *Macroscopic analysis of kidneys at 7 days after unilateral ureteral obstruction. A: Macroscopic photographs of kidney sections stained with hematoxylin-eosin. Control and obstructed kidneys from wild-type (Timp-3$^{+/+}$) and knockout (Timp-3$^{-/-}$) mice were fixed, sectioned, and stained. Solid lines indicate sections of the renal cortex, and dotted lines indicate sections of the medulla. B: The ratio of the thickness of the medulla to that of the cortex is shown. The thickness was measured with hematoxylin-eosin–stained sections of control and obstructed kidneys from Timp-3$^{+/+}$ and Timp-3$^{-/-}$ mice. C: Ratios of the renal parenchymal area to the total renal area are shown. Areas were measured with hematoxylin-eosin–stained sections of obstructed kidneys from Timp-3$^{+/+}$ and Timp-3$^{-/-}$ mice. Values are the mean ± SD.* N = *3 for each group.* *p < *0.05 compared with wild-type kidneys. CTR, control; Ob, obstructed.*

trophic or distended after UUO, renal sections were stained with hematoxylin-eosin. Macroscopically, the renal tissues of sections from KO animals were thinner than those of WT animals, indicating that the renal tissues of KO mice were distended rather than hypertrophic. Contralateral, non-ligated kidneys from KO mice were indistinguishable from WT kidneys. Obstructed kidneys of WT mice appeared to exhibit three layers, cortex, outer medulla, and inner medulla. In contrast, the border between the outer and inner medulla was unclear in obstructed kidneys from KO mice, indicating severe hydronephrosis (Fig. 4A). To determine the ratio of renal medulla to cortex, the thickness of each layer was determined. The medulla-to-cortex ratio was significantly smaller in obstructed kidneys in the KO mice than in those in WT mice. The ratio was not different between the unligated control kidneys of KO and WT mice (Fig. 4B). The ratio of the renal parenchymal tissue area to the total tissue area was also smaller in obstructed KO kidneys than that in WT kidneys (Fig. 4C). These findings indicate that Timp-3-deficiency accelerates hydronephrosis and the thinning of renal parenchymal tissue, especially the renal medulla.

Histological Analysis

To examine the histological changes of the renal cortex in KO mice, sections were stained by hematoxylin-eosin. There were no differences in the control kidneys between WT and KO mice (Fig. 5A, B). After 7 days of UUO, dilation of tubules due to hydronephrosis and widening of the interstitial space of the renal cortex were noted in both WT and KO kidneys (Fig. 5C, D). To evaluate the fibrotic change after UUO, sections were stained with Masson trichrome reagents (Fig. 5E, F). Sections from obstructed WT and KO kidneys exhibited comparable levels of fibrotic change in the interstitial space. Since tubulointerstitial fibrosis is characterized by the accumulation of myofibroblasts as well as ECM (*30*), sections were stained with an α-SMA–specific antibody to visualize myofibroblasts (Fig. 6A). This demonstrated the presence of myofibroblasts in both obstructed kidneys of WT and KO. However, the α-SMA score/section was not signifi-

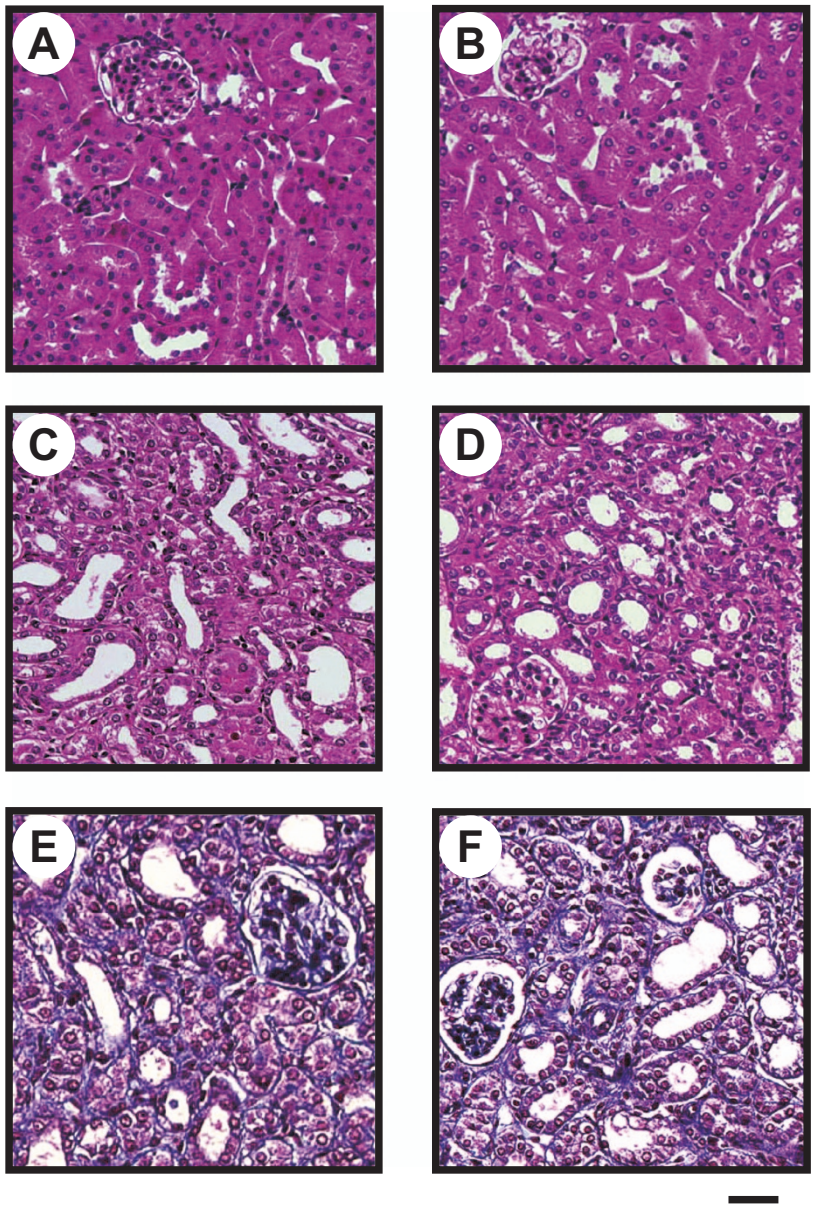

Fig. 5. *Photomicrographs of the renal cortex stained with hematoxylin-eosin (A–D) and Masson trichrome (E, F). Wild-type control kidney (A), Timp-3$^{-/-}$ control kidney (B), and wild-type kidney 7 days after unilateral ureteral obstruction (UUO) (C), and Timp-3$^{-/-}$ kidney 7 days after UUO (D). Wild-type kidney 7 days after UUO (E) and Timp-3$^{-/-}$ kidney 7 days after UUO (F). Scale bar, 50 μm.*

cantly different between WT and KO (Fig 6B), suggesting that the lack of Timp-3 did not influence the accumulation of α-SMA–positive myofibroblasts in interstitial space. These findings indicate that Timp-3-deficiency did not markedly affect fibrosis in the renal cortex after UUO.

In Situ Zymography and TGF-β Expression

The results of *in situ* zymography are shown in Fig. 7. *In situ* gelatinolytic activity after 1 h incubation at 37°C using gelatin films revealed negligible levels of gelatinolytic activity in the control kidneys of WT and KO mice (Fig. 7A, B). In comparison, gelatinolytic activity was increased in both the cortex and medulla at 7 days after UUO in the WT kidneys (Fig. 7C). A markedly strong activity was demonstrated in the KO kidneys at 7 days after UUO (Fig. 7D). The gelatinolytic activities were almost completely abolished on the gelatin films coated with *o*-phenanthroline, suggesting that the activities are dependent on MMP (not shown). These findings indicate that the gelatinolytic activity after UUO is largely inhibited

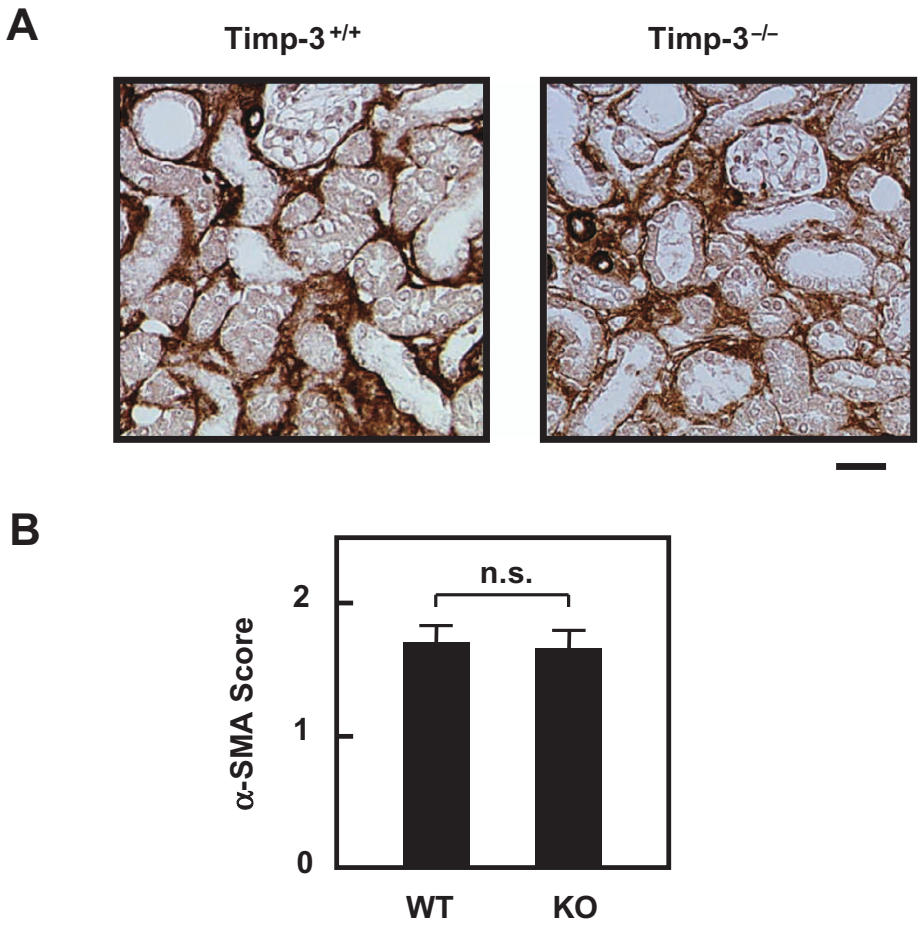

Fig. 6. *Immunohistochemical detection and quantitative analysis of α-smooth muscle actin (α-SMA) in kidneys 7 days after unilateral ureteral obstruction (UUO). A: Light-field photomicrographs of cortical regions stained with mouse monoclonal anti–α-SMA antibody in obstructed Timp-3 $^{+/+}$ and Timp-3 $^{-/-}$ kidneys. B: α-SMA score of the kidney cortex of mice at 7 days after UUO. Matrix scores of Timp-3 $^{+/+}$ (WT) and Timp-3 $^{-/-}$ (KO) were determined as described in the Methods section. Values are the mean ± SD.* N = *4 for each group. Scale bar, 50 μm.*

by Timp-3. TGF-β is considered to be an important mediator of the progression of tubulointerstitial fibrosis in UUO models (*17*, *28*, *31*). We therefore examined the expression of TGF-β in the kidneys of KO mice at 7 days after UUO. Northern blot analysis demonstrated that the expression of TGF-β in the obstructed KO kidneys was approximately 2.3-fold that in the obstructed WT kidneys (Fig. 7E). This finding suggests that the degradation of ECM by uninhibited gelatinolytic activities in the KO kidneys may be compensated by the increased synthesis induced by TGF-β.

Discussion

In this study, we created Timp-3–deficient mice using an ES cell gene targeting technique. It has been reported that Timp-3-deficiency disrupts the Timp/MMP balance to favor ECM degradation and results in enlarged alveolar spaces in the lung (*32*). Timp-3-deficiency is also shown to disrupt the matrix homeostasis and the balance of inflammatory mediators, leading to cardiac dilatation and dysfunction (*33*, *34*). However, the role of Timp-3 on vascular resistance or in the kidney, in which Timp-3 is expressed at the highest levels (*6*, *35*), is still to be determined. We therefore investigated the role of Timp-3 on blood pressure and examined the function of Timp-3 in the kidney using a model of UUO that mimics obstructive nephritis leading to tubulointerstitial fibrosis.

Blood pressure is generally determined by both perivascular resistance and cardiac output. Perivascular fibrosis which increases vascular resistance is considered to raise the blood pressure (*36*, *37*). Therefore, the lack of MMP-inhibition in KO mice is expected to reduce perivascular fibrosis and lower the blood pressure. In the present study, however, the blood pressure of KO mice did not significantly differ from that of WT mice, indicating that Timp-3 deficiency does not substantially affect the vascular resistance. It is possible that interventions for blood pressure, such as infusion of angiotensin

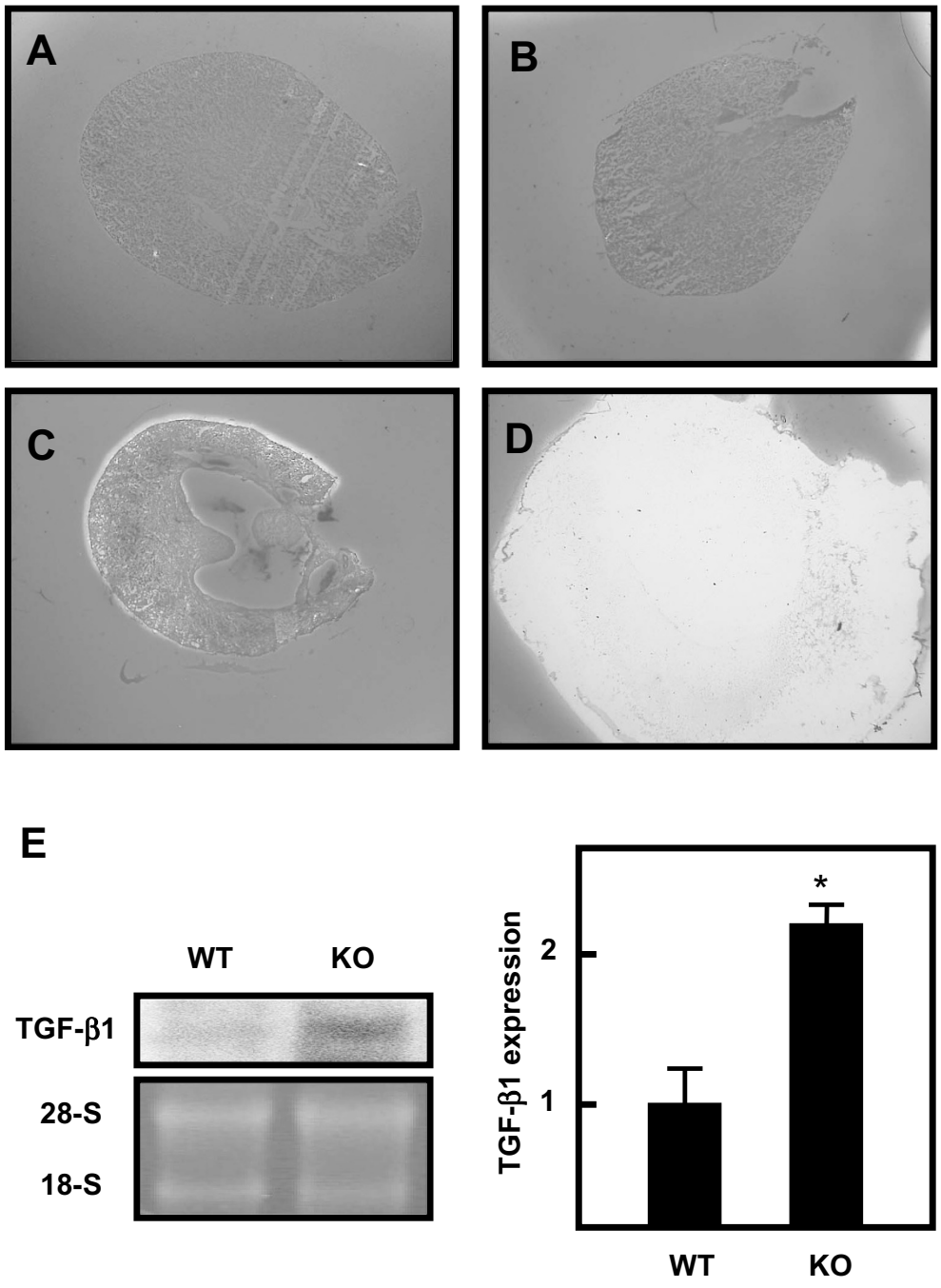

Fig. 7. *Gelatinolytic activity and TGF-β expression at 7 days after unilateral ureteral obstruction (UUO).* In situ *zymography for detection of gelatinolytic activities in kidneys of wild-type (A and C) and Timp-3$^{-/-}$ (B and D) mice. A and B: Control kidneys. C and D: Kidneys at 7 days after obstruction. E: Northern blot analysis of TGF-β expression in total RNA (10 μg) isolated from wild-type (WT) and Timp-3$^{-/-}$ (KO) kidneys 7 days after UUO. The 28-S and 18-S rRNA bands from the ethidium bromide–stained gel are shown. The graph shows the mean band density. Values are the mean±SD.* N = *3 for each group.* *$p < 0.05$ *compared with WT kidneys after UUO.*

II, reveal differences of blood pressure between WT and KO by affecting the degree of vascular fibrosis and resistance.

On the other hand, there were no evident differences in the degree of fibrosis in the renal cortex after UUO between WT and KO animals. However, the medulla-to-cortex ratio differed significantly between these mice. The ratio of the thickness of the renal medulla to that of the cortex in Timp-3–deficient mice was less than that in WT mice, and the ratio of

the renal parenchymal area to total area was less in the KO kidneys than in the WT kidneys. These findings suggest that Timp-3-deficiency affects the structure of the renal medulla rather than the cortex. The reduction of the renal parenchymal area in KO mice may be due to the atrophic change in the renal medulla. It is also possible that a structural weakness of the medulla resulted in severe compression and distension of renal parenchymal tissues of Timp-3–deficient kidneys after UUO.

In situ zymography, a technique that reveals the MMP activities in tissue sections, demonstrated that there was a huge elevation of gelatinolytic activity in the obstructed kidneys of KO mice, compared with that in the obstructed WT kidneys. This is consistent with the lack of MMP-inhibitory activity. Considering that fibrosis results from excessive production or reduced degradation of ECM, a lack of MMP-inhibition would be expected to reduce interstitial fibrosis. However, the degree of fibrosis did not appear to be reduced in the cortex of the KO kidneys. One possible explanation for this is enhanced expression of TGF-β in the renal tissue, which will accelerate the synthesis of ECM. Connective tissue growth factor (CTGF) is thought to be a mediator of the fibrogenic properties of TGF-β (*38*). Alternatively, there may be a compensation for Timp-3-deficiency by other members of the Timp family or plasminogen activator inhibitor-I. However, this appears unlikely because the gelatinolytic activity *in vivo* was markedly enhanced in the obstructed KO kidneys. It is also possible that the gelatinolytic activity in renal tissue does not substantially contribute to the fibrotic response induced by UUO.

In summary, despite the high level of expression of Timp-3 in the kidneys of mice, kidneys of Timp-3–deficient mice do not show alterations without interventions. However, after UUO, KO kidneys develop severe hydronephrosis with thinning of the renal tissues. It is possible that macrostructural change in Timp-3–deficient kidneys occurred by a mechanism other than fibrotic change in the renal cortex caused by the imbalance of MMP and Timp. In the future, assays of apoptosis and macrophage infiltration will be important in clarifying the mechanisms of hydronephrosis in the Timp-3–deficient kidney.

Acknowledgements

We are grateful to Dr. S. Mizuno and Dr. Y. Nagasawa for helpful discussion. We are also grateful to Ms. T. Kaimoto for her technical and secretarial assistance.

References

1. Diamond JA, Phillips RA: Hypertensive heart disease. *Hypertens Res* 2005; **28**: 191–202.
2. Firestein GS: Evolving concepts of rheumatoid arthritis. *Nature* 2003; **423**: 356–361.
3. Tsunemi K, Takai S, Miyazaki M, *et al*: Possible roles of angiotensin II–forming enzymes, angiotensin converting enzyme and chymase-like enzyme, in the human aneurysmal aorta. *Hypertens Res* 2002; **25**: 817–822.
4. Iwashima Y, Horio T, Kuroda S, Takishita S, Kawano Y: Influence of plasma aldosterone on left ventricular geometry and diastolic function in treated essential hypertension. *Hypertens Res* 2002; **25**: 49–56.
5. Pavloff N, Staskus PW, Kishnani NS, Hawkes SP: A new inhibitor of metalloproteinases from chicken: ChIMP-3. A third member of the TIMP family. *J Biol Chem* 1992; **267**: 17321–17326.
6. Leco KJ, Khokha R, Pavloff N, Hawkes SP, Edwards DR: Tissue inhibitor of metalloproteinases-3 (TIMP-3) is an extracellular matrix–associated protein with a distinctive pattern of expression in mouse cells and tissues. *J Biol Chem* 1994; **269**: 9352–9360.
7. Fedak PW, Verma S, Weisel RD, Li RK: Cardiac remodeling and failure from molecules to man (Part II). *Cardiovasc Pathol* 2005; **14**: 49–60.
8. Amour A, Slocombe PM, Murphy G, *et al*: TNF-alpha converting enzyme (TACE) is inhibited by TIMP-3. *FEBS Lett* 1998; **435**: 39–44.
9. Bian J, Wang Y, Sun Y, *et al*: Suppression of *in vivo* tumor growth and induction of suspension cell death by tissue inhibitor of metalloproteinases (TIMP)-3. *Carcinogenesis* 1996; **17**: 1805–1811.
10. Cruz-Munoz W, Kim I, Khokha R: TIMP-3 deficiency in the host, but not in the tumor, enhances tumor growth and angiogenesis. *Oncogene* 2006; **25**: 650–655.
11. Baker AH, George SJ, Zaltsman AB, Murphy G, Newby AC: Inhibition of invasion and induction of apoptotic cell death of cancer cell lines by overexpression of TIMP-3. *Br J Cancer* 1999; **79**: 1347–1355.
12. Baker AH, Zaltsman AB, George SJ, Newby AC: Divergent effects of tissue inhibitor of metalloproteinase-1, -2, or -3 overexpression on rat vascular smooth muscle cell invasion, proliferation, and death *in vitro*. TIMP-3 promotes apoptosis. *J Clin Invest* 1998; **101**: 1478–1487.
13. Bond M, Murphy G, Baker AH, *et al*: Localization of the death domain of tissue inhibitor of metalloproteinase-3 to the N terminus. Metalloproteinase inhibition is associated with proapoptotic activity. *J Biol Chem* 2000; **275**: 41358–41363.
14. Qi JH, Ebrahem Q, Anand-Apte B, *et al*: A novel function for tissue inhibitor of metalloproteinases-3 (TIMP3): inhibition of angiogenesis by blockage of VEGF binding to VEGF receptor-2. *Nat Med* 2003; **9**: 407–415.
15. Weber BH, Vogt G, Pruett RC, Stohr H, Felbor U: Mutations in the tissue inhibitor of metalloproteinases-3 (TIMP3) in patients with Sorsby's fundus dystrophy. *Nat Genet* 1994; **8**: 352–356.
16. Pulido J, Sanders D, Winters JL, Klingel R: Clinical outcomes and mechanism of action for rheopheresis treatment of age-related macular degeneration (AMD). *J Clin Apher* 2005; **20**: 185–194.
17. Klahr S, Morrissey J: Obstructive nephropathy and renal fibrosis. *Am J Physiol Renal Physiol* 2002; **283**: F861–F875.
18. Bascands JL, Schanstra JP: Obstructive nephropathy: insights from genetically engineered animals. *Kidney Int* 2005; **68**: 925–937.

19. Saito K, Ishizaka N, Nagai R, *et al*: Role of aberrant iron homeostasis in the upregulation of transforming growth factor-β1 in the kidney of angiotensin II–induced hypertensive rats. *Hypertens Res* 2004; **27**: 599–607.
20. Oda T, Jung YO, Eddy AA, *et al*: PAI-1 deficiency attenuates the fibrogenic response to ureteral obstruction. *Kidney Int* 2001; **60**: 587–596.
21. Engelmyer E, van Goor H, Edwards DR, Diamond JR: Differential mRNA expression of renal cortical tissue inhibitor of metalloproteinase-1, -2, and -3 in experimental hydronephrosis. *J Am Soc Nephrol* 1995; **5**: 1675–1683.
22. Kim H, Oda T, Lopez-Guisa J, Eddy AA, *et al*: TIMP-1 deficiency does not attenuate interstitial fibrosis in obstructive nephropathy. *J Am Soc Nephrol* 2001; **12**: 736–748.
23. Apte SS, Olsen BR, Murphy G: The gene structure of tissue inhibitor of metalloproteinases (TIMP)-3 and its inhibitory activities define the distinct TIMP gene family. *J Biol Chem* 1996; **271**: 2874.
24. Bronson SK, Plaehn EG, Kluckman KD, Hagaman JR, Maeda N, Smithies O: Single-copy transgenic mice with chosen-site integration. *Proc Natl Acad Sci U S A* 1996; **93**: 9067–9072.
25. Nagatoya K, Moriyama T, Hori M, *et al*: Y-27632 prevents tubulointerstitial fibrosis in mouse kidneys with unilateral ureteral obstruction. *Kidney Int* 2002; **61**: 1684–1695.
26. Mizuno S, Matsumoto K, Nakamura T: Hepatocyte growth factor suppresses interstitial fibrosis in a mouse model of obstructive nephropathy. *Kidney Int* 2001; **59**: 1304–1314.
27. Moriyama T, Kawada N, Hori M, *et al*: Up-regulation of HSP47 in the mouse kidneys with unilateral ureteral obstruction. *Kidney Int* 1998; **54**: 110–119.
28. Mizuno S, Matsumoto K, Kurosawa T, Mizuno-Horikawa Y, Nakamura T: Reciprocal balance of hepatocyte growth factor and transforming growth factor-beta 1 in renal fibrosis in mice. *Kidney Int* 2000; **57**: 937–948.
29. Muramatsu M, Takai S, Miyazaki M: Detections of matrix metalloproteinases activities and localization by film *in situ* zymography (FIZ). *Nippon Yakurigaku Zasshi* 2003; **121**: 113–118 (in Japanese).
30. Lan HY, Mu W, Morishita R, *et al*: Inhibition of renal fibrosis by gene transfer of inducible Smad7 using ultrasound-microbubble system in rat UUO model. *J Am Soc Nephrol* 2003; **14**: 1535–1548.
31. Kuncio GS, Neilson EG, Haverty T: Mechanisms of tubulointerstitial fibrosis. *Kidney Int* 1991; **39**: 550–556.
32. Leco KJ, Waterhouse P, Khokha R, *et al*: Spontaneous air space enlargement in the lungs of mice lacking tissue inhibitor of metalloproteinases-3 (TIMP-3). *J Clin Invest* 2001; **108**: 817–829.
33. Fedak PW, Smookler DS, Khokha R, *et al*: TIMP-3 deficiency leads to dilated cardiomyopathy. *Circulation* 2004; **110**: 2401–2409.
34. Ishimitsu T, Kobayashi T, Matsuoka H, *et al*: Protective Effects of an angiotensin II receptor blocker and a long-acting calcium channel blocker against cardiovascular organ injuries in hypertensive patients. *Hypertens Res* 2005; **28**: 351–359.
35. Wu I, Moses MA: Cloning and expression of the cDNA encoding rat tissue inhibitor of metalloproteinase-3 (TIMP-3). *Gene* 1996; **168**: 243–246.
36. Asai M, Monkawa T, Saruta T, *et al*: Spironolactone in combination with cilazapril ameliorates proteinuria and renal interstitial fibrosis in rats with anti–Thy-1 irreversible nephritis. *Hypertens Res* 2004; **27**: 971–978.
37. Sato A, Saruta T: Aldosterone-induced organ damage: plasma aldosterone level and inappropriate salt status. *Hypertens Res* 2004; **27**: 303–310.
38. Yokoi H, Mukoyama M, Nagae T, *et al*: Reduction in connective tissue growth factor by antisense treatment ameliorates renal tubulointerstitial fibrosis. *J Am Soc Nephrol* 2004; **15**: 1430–1440.